NMR Spectroscopy

Deutsche Ausgabe: DOI: 10.1002/ange.201910118
Internationale Ausgabe: DOI: 10.1002/anie.201910118

Metal-Chelated Polymer Nanodiscs for NMR Studies

*Nathaniel Z. Hardin[+], Vojč Kocman[+], Giacomo M. Di Mauro, Thirupathi Ravula, and Ayyalusamy Ramamoorthy**

Abstract: *Paramagnetic relaxation enhancement (PRE) is commonly used to speed up spin lattice relaxation time (T_1) for rapid data acquisition in NMR structural studies. Consequently, there is significant interest in novel paramagnetic labels for enhanced NMR studies on biomolecules. Herein, we report the synthesis and characterization of a modified poly(styrene-co-maleic acid) polymer which forms nanodiscs while showing the ability to chelate metal ions. Cu^{2+}-chelated nanodiscs are demonstrated to reduce the T_1 of protons for both polymer and lipid-nanodisc components. The chelated nanodiscs also decrease the proton T_1 values for a water-soluble DNA G-quadruplex. These results suggest that polymer nanodiscs functionalized with paramagnetic tags can be used to speed-up data acquisition from lipid bilayer samples and also to provide structural information from water-soluble biomolecules.*

Nanodiscs are comprised of a discoidal lipid bilayer stabilized by an amphiphilic belt comprised of either peptidic based or polymer based molecules.[1–4] The introduction of amphiphilic polymers that form lipid nanodiscs has most notably contributed to the study of membrane proteins (MPs) and allows for their functional and structural study in a tunable native-like membrane environment.[5–10] While polymer nanodiscs are the youngest of the nanodisc field, they are showing great potential due to the simplicity of their synthesis, their diverse chemical tunability, and their ability to directly extract membrane proteins from their cellular environment at practical cost.[5–7,9,11–22] Nanodiscs are a useful tool for NMR spectroscopy since their size can be tuned to conditions favorable to both solution and solid-state NMR. Additionally, nanodiscs were shown to align in the presence of the magnetic field which can provide additional useful structural information.[8,19,23] Despite these advantages the fundamental challenges related to poor NMR sensitivity still remain, requiring long acquisition times and high sample concentrations.[24] In this study we focused on the synthesis of a nanodisc-forming metal-chelated polymer and its use as a paramagnetic relaxation enhancement (PRE) system. We show that the polymer was able to decrease longitudinal relaxation times (T_1) of nanodisc and DNA with a minimum adverse transverse relaxation shortening (T_2), which is ideal for fast NMR data acquisition.[25–30] We sought a simple method of preparing polymer nanodiscs modified with a stable metal chelator, 2-aminoethyl-monoamide-DOTA (DOTA, Figure 1a), attached to the polymer belt for use as a system for T_1 relaxation enhancement. Designing polymer nanodiscs in such a way has two major advantages over previously reported lipid-chelator methods.[26,27] First, the position of the chelator on the nanodisc belt removes potentially detrimental effects of interacting DOTA-metal complexes in very close proximity to membrane associated biomolecules, while leaving a native like membrane environment. Secondly, the facile polymer preparation allows for exploitation of the paramagnetic effects of metal ions complexed by nanodiscs without the need for costly metal complexed lipids. This strategy would also enable the use of PRE in the structural studies of membrane proteins.[28,31,32]

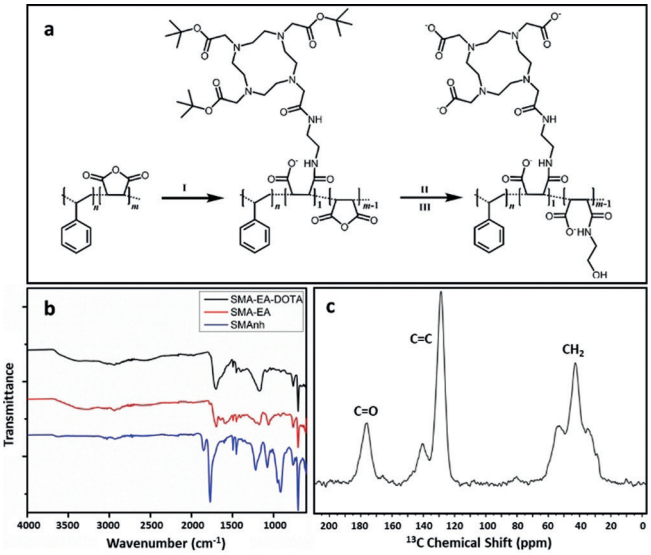

Figure 1. a) Reaction scheme of SMA-EA-DOTA synthesis: I) 2-aminoethyl-monoamide-DOTA-tris(*tert*-butyl ester), NMP, triethylamine; II) ethanolamine, triethylamine; III) TFA deprotection. b) FT-IR spectra of polymers. c) ^{13}C CP-MAS solid-state NMR spectrum of SMA-EA-DOTA polymer. FT-IR and NMR spectra were recorded with polymer powder samples.

Here we report the synthesis of a modified poly(styrene-co-maleic acid) (SMA) derivative called SMA-EA-DOTA which is engineered with a metal chelator and forms lipid-nanodiscs. SMA-EA-DOTA polymer was synthesized similarly to SMA-EA polymer, which has been previously reported to form stable nanodiscs and is used as a comparative

[*] N. Z. Hardin,[+] V. Kocman,[+] G. M. Di Mauro, T. Ravula, Prof. A. Ramamoorthy
Biophysics Program and Department of Chemistry
University of Michigan
Ann Arbor, MI 48109-1055 (USA)
E-mail: ramamoor@umich.edu
[+] These authors contributed equally to this work

Supporting information and the ORCID identification number(s) for the author(s) of this article can be found under https://doi.org/10.1002/anie.201910118.

system in this study. To synthesize the polymer, we used a low molecular weight ($M_n \approx 1600\ g\,mol^{-1}$) poly(styrene-co-maleic anhydride) (SMAnh) as the starting material.[19] The chemical modification of the SMAnh includes on average one DOTA chelator molecule per polymer chain modification (Figure 1a; see methods section in the Supporting Information).

The successful polymer modification was confirmed using FT-IR and ^{13}C-CP-MAS solid-state NMR experiments on polymer powders (Figure 1b,c). The FT-IR spectrum shows a clear C=O stretching frequency shift from 1770 cm^{-1} to 1702 cm^{-1} indicating a change from an anhydride to an amide, which is further confirmed by the ^{13}C C=O NMR signal at 176 ppm. The ability of the polymer to form lipid nanodiscs with DMPC was established using dynamic light scattering (DLS), static light scattering (SLS), size-exclusion chromatography (SEC), and transmission electron microscopy (TEM) (Figure 2). The nanodiscs were shown to be size tunable at differing weight ratios (from 1:1 to 3:1 w/w) of polymer to DMPC by the shift in elution volume in SEC of the nanodiscs peak from 65 to 87 mL (Figures 2a and S1). DLS shows the formation of small particles of ≈8 nm diameter which is further confirmed by the presence of small disc-shaped particles in TEM (Figure 2b,c). These results show that the addition of DOTA-units to the SMA-EA polymer does not significantly change its nanodisc formation ability. To further establish the addition of the DOTA-units to the polymer we compared the metal ion stability of the SMA-EA-DOTA to previously studied SMA-EA by monitoring polymer nanodiscs precipitation upon the addition of copper(II) ions (Figure 2d). The resulting metal ion stability showed the expected increase in the Cu^{2+} tolerance as compared to SMA-EA nanodiscs due to the addition of the DOTA-units sequestering the Cu^{2+} ions.

Furthermore, the polymer SMA-EA-DOTA showed similar size control and pH stability properties as compared to SMA-EA indicating that the addition of roughly one DOTA chelator per chain did not introduce any significant change in the lipid-nanodiscs forming properties of the polymer (Figure S2).

NMR samples were prepared using a polymer:DMPC ratio of 3:1 w:w (6 mg:2 mg) to form nanodiscs of size ≈8 nm (diameter) as observed from DLS results. The resulting nanodiscs were purified using SEC and concentrated to 1 mL using a 10 kDa filter. As shown in Figure 3, most of the peaks

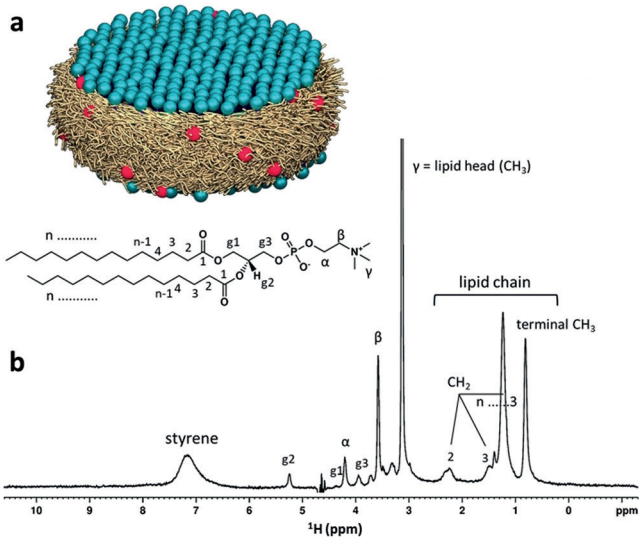

Figure 3. a) Schematic of SMA-EA-DOTA polymer-nanodiscs with lipid head, DOTA functional groups, and polymer represented in blue, red, and brown, respectively. A chemical structure of a lipid molecule with assignment is shown. b) ^{1}H NMR spectrum of a polymer nanodiscs recorded on a 500 MHz NMR spectrometer at 25 °C with assignment of lipid and styrene protons.

in the proton NMR spectrum of the functionalized nanodiscs were assigned. To demonstrate the PRE effect on relaxation parameters, we chose to monitor the well resolved and minimally overlapped peaks assigned to styrene (7.2 ppm), lipid-head (3.2 ppm), CH_2 (1.3 ppm) and CH_3 (0.9 ppm) protons.[33] We used a standard inversion-recovery RF pulse sequence and added an excitation sculpting with selective pulses for water suppression as described elsewhere.[34] We determined the T_1 times of these four ^{1}H peaks (Figures 4 and S3–S9) in the absence and presence of differing concentrations of chelated Cu^{2+} metal ions. In the absence of Cu^{2+} ions, protons from styrene, lipid head, CH_2 and CH_3 groups exhibited T_1 values of 1.3, 0.5, 0.7 and 0.7 s, respectively (Figure 4). Next, we determined T_1 relaxation rates of nanodiscs samples with a Cu^{2+} concentration ranging from 10 μM to 3 mM (Figures 4 and S3–S9). We observed a slight decrease in T_1 values at concentrations of 10 and 100 μM Cu^{2+}, and a significant drop in T_1 values were observed at >250 μM Cu^{2+}, with T_1 relaxation values approaching saturation at

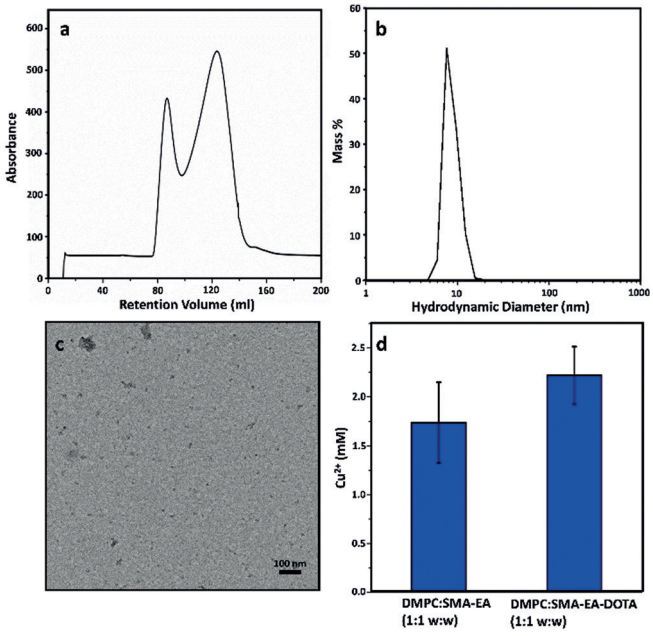

Figure 2. Nanodiscs prepared using 3:1 w/w polymer:lipid for (a) to (c) and 1:1 w/w for (d). a) SEC profile of SMA-EA-DOTA nanodiscs. b) DLS profile of purified nanodiscs. c) TEM image showing small nanodiscs; scale bar represents 100 nm. d) SMA-EA and SMA-EA-DOTA nanodiscs tolerance/precipitation in the presence of differing Cu^{2+} concentrations.

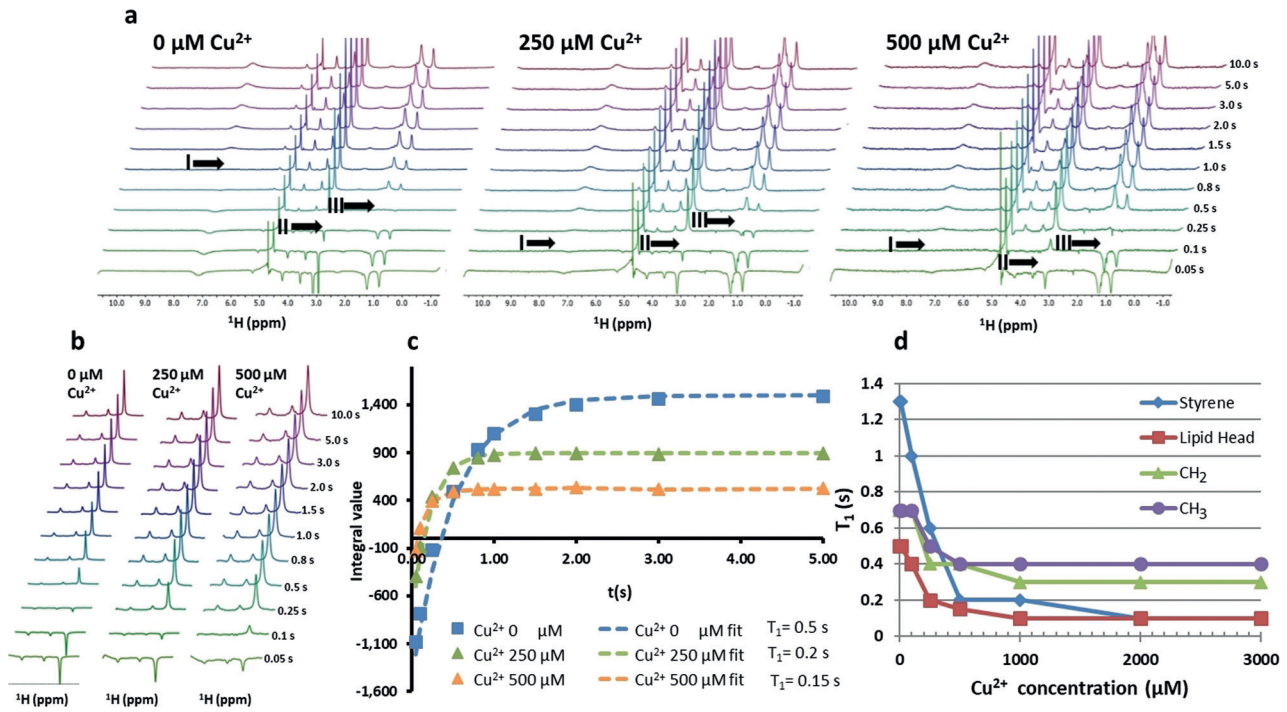

Figure 4. Inversion recovery experiments to measure T_1 of protons from SMA-EA-DOTA nanodiscs. a) Inversion recovery experiments recorded on a SMA-EA-DOTA nanodiscs at 0, 250 and 500 μM Cu^{2+} concentrations are shown. Roman numerals I, II and III indicate where the intensities of styrene, lipid head and lipid chain peaks, respectively, are close to or zero. b) Close up of the lipid head region of the inversion recovery spectra. c) Inversion recovery data and fit for the lipid head peak at 0, 250 and 500 μM Cu^{2+} concentrations. d) T_1 times of styrene, lipid head and lipid chain peaks and their dependence on [Cu^{2+}] concentration.

≈0.5 mM Cu^{2+}. The control (SMA-EA nanodiscs-no chelator) showed no decrease of T_1 times upon the addition of copper (Figure S10). SMA-EA was also incompatible with higher Cu^{2+} concentrations due to precipitation of the polymer. The maximum T_1 enhancement with ensured stability was achieved at 2 mM Cu^{2+}, as the calculated DOTA concentration was ≈4.0 mM. Removal of non-nanodiscs forming polymer in solution by SEC reduces the effective concentration of DOTA in the purified polymer nanodiscs, therefore 2 mM Cu^{2+} was chosen for our studies as a maximum copper concentration with ensured chelation. Based on the PRE experiments we found that copper chelated nanodiscs showed the greatest T_1 relaxation enhancement for the styrene moiety, due to the proximity of styrene to the Cu-DOTA-units (Figure 4). The second most effected region is the quaternary ammonium lipid head CH_3 group. The lesser PRE effect observed, as compared to the styrene, is due to an average much greater distance from the Cu-DOTA-units to the lipid head CH_3. Interestingly, the PRE effect for the lipid head CH_3 protons is comparable to that for the CH_2 and CH_3 protons of the lipid chain which are on average closer to the Cu-DOTA-units compared to the lipid head group. This is most likely due to the fact that the lipid head groups can undergo both intra-discs and inter-discs PRE enhancements as they are solution exposed, whereas the lipid chain protons can only undergo intra-disc PRE due to a lack of solvent exposure.

As a proof of principle of widening the applications of polymer nanodiscs from mainly a membrane mimetic system to also a stable, minimally interacting system for fast NMR acquisition of water-soluble biomolecules, we decided to test the polymer nanodisc PRE effect on a DNA oligonucleotide from the human telomere region (wtTel23, 5′-TAGGG-$(TTAGGG)_3$-3′, Figure 5). We reasoned that there should be no interactions between the negatively charged polymer and the negatively charged DNA. The wtTel23 sequence is known to form a well characterized G-quadruplex in presence of K^+ ions.[35] The wtTel23 G-quadruplex was folded in the presence of 100 mM KCl and we confirmed that the wtTel23 oligonucleotide used in this study adopted the previously reported hybrid-1 G-quadruplex topology by a comparison of ^{1}H-NMR spectra to published literature (Figure S11).[35] After the addition of the folded wtTel23 to the copper chelated polymer nanodiscs the non-overlapped NMR fingerprint showed no significant change in the ^{1}H-NMR spectrum indicating the retention of hybrid-1 G-quadruplex topology (Figure S12).

A G-quadruplex fold is characterized by stacked G-quartets which are planar arrangements of four guanine residues (Figure 5). In each G-quartet, the imino protons of guanine residues form a hydrogen bond with an oxygen atom of a neighboring guanine residue. Critically, the oxygen atoms inside a G-quartet must be stabilized by a cation such as Na^+ or K^+ for the G-quadruplex to be stable. In a G-quadruplex, the G-quartets are arranged in such a way that the imino protons can be considered as the "inside" of a G-quadruplex. The H8 protons and sugar moieties of guanine residues involved in G-quartets as well as residues not involved in G-

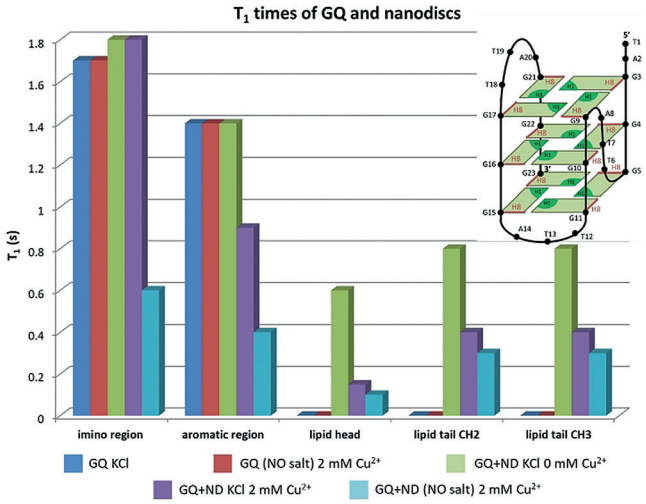

Figure 5. T_1 times of signals from the imino and aromatic regions of the G-quadruplex (GQ) and lipid head, CH_2 and CH_3 signals of the nanodiscs in presence or absence of Cu^{2+} and KCl salt. Top, right: a representation of the structure of the wtTel23 G-quadruplex. The black circle shows the position of a residue, green squares represent guanines located in G-quartets, the position of imino protons inside guanine residues is labeled with dark green and the red line shows on which side of the guanine residue the H8 proton is located.

quartets form the so called solvent exposed "outside" of a G-quadruplex. After the addition of 2 mM Cu^{2+} cleated polymer nanodiscs to the DNA we observed no effect on the T_1 times of imino protons and a $\approx$0.5 s decrease in the T_1 times of the signals in the aromatic region (Figure 5). The sugar region was overlapped with the signals from the nanodiscs and could not be used for accurate T_1 determination. This T_1 data suggest that the wtTel23 interacts with the nanodiscs by its groove or loop regions and not through stacking on the nanodiscs by the top or bottom G-quartet. Such a model of interactions is also supported by saturation transfer difference (STD) NMR experiments (Figure S13). We observed a clear transfer of magnetization from the lipid head protons to the sugar and aromatic protons of the wtTel23 G-quadruplex and a negligible transfer to the imino protons of the G-quadruplex. Interestingly, upon the removal of excess salt, both the imino and aromatic proton resonances were shown to have a 3-fold reduction in their T_1 times. We believe that the KCl salt reduces the interactions between the G-quadruplex and the nanodisc due to the salt charge screening between the DNA and the lipid heads. This decreased interaction is also reflected in the observed reduction in the PRE effect. Removing the salt increases the strength of the interactions between the nanodiscs and G-quadruplexes and consequently increases the PRE effect (Figure 5). This interesting result suggests that DOTA functionalized nanodiscs could potentially be used to structurally and dynamically probe surfaces of biomolecules similar to previously applied solvent PRE techniques.[36–40]

In conclusion, we have demonstrated the functionalization of a metal-chelating polymer and its ability to form nanodiscs, which can be used as a stable, relatively non-interacting system for PRE enhancement of biomolecules for fast NMR acquisition. We show, using inverse recovery experiments, up to a 7× decrease of T_1 rates of polymer-lipid nanodiscs. We also show the compatibility of nanodiscs and structured DNA molecules (G-quadruplexes) and up to 3× reduction in T_1 times. We expect this approach to be valuable in the NMR structural studies of large size RNA that exhibit a very long T_1 values for protons;[41] and could enable multidimensional NMR experimental studies on membrane-associated peptides and proteins that may not be available in large quantity and/or sensitive to heat for long data acquisition. This system coupled with recent developments in our lab to measure RDCs[23] will yield an useful tool for fast NMR acquisition in the study of biomolecules as well as the already known application in MP research. This study also creates potential avenues to use the paramagnetic nature of the chelated polymer nanodiscs for dynamic nuclear polarization (DNP) solid-state NMR experiments[31,32,42–45] to overcome the sensitivity issues in studying membrane proteins. We expect that the reported novel polymer design would enable multi-labeling to utilize the benefits of PRE, ^{19}F and DNP approaches for distance measurements on membrane proteins by solid-state NMR spectroscopy.

Acknowledgements

This study was supported by funds from NIH (GM084018 to A.R.).

Conflict of interest

The authors declare no conflict of interest.

Keywords: metal chelation · NMR spectrocopy · paramagnetic relaxation enhancement (PRE) · polymer nanodiscs · T_1 enhancement

How to cite: *Angew. Chem. Int. Ed.* **2019**, *58*, 17246–17250
Angew. Chem. **2019**, *131*, 17406–17410

[1] I. G. Denisov, S. G. Sligar, *Nat. Struct. Mol. Biol.* **2016**, *23*, 481.
[2] I. G. Denisov, S. G. Sligar, *Chem. Rev.* **2017**, *117*, 4669–4713.
[3] S. C. Lee, T. J. Knowles, V. L. Postis, M. Jamshad, R. A. Parslow, Y. P. Lin, A. Goldman, P. Sridhar, M. Overduin, S. P. Muench, T. R. Dafforn, *Nat. Protoc.* **2016**, *11*, 1149–1162.
[4] M. C. Orwick, P. J. Judge, J. Procek, L. Lindholm, A. Graziadei, A. Engel, G. Grobner, A. Watts, *Angew. Chem. Int. Ed.* **2012**, *51*, 4653–4657; *Angew. Chem.* **2012**, *124*, 4731–4735.
[5] T. Ravula, N. Z. Hardin, S. K. Ramadugu, S. J. Cox, A. Ramamoorthy, *Angew. Chem. Int. Ed.* **2018**, *57*, 1342–1345; *Angew. Chem.* **2018**, *130*, 1356–1359; Corrigendum: T. Ravula, N. Z. Hardin, S. K. Ramadugu, S. J. Cox, A. Ramamoorthy, *Angew. Chem. Int. Ed.* **2019**, *58*, 13185–13185; *Angew. Chem.* **2019**, *131*, 13319–13319.
[6] T. Ravula, N. Z. Hardin, G. M. Di Mauro, A. Ramamoorthy, *Eur. Polym. J.* **2018**, *108*, 597–602.
[7] J. M. Dörr, S. Scheidelaar, M. C. Koorengevel, J. J. Dominguez, M. Schäfer, C. A. van Walree, J. A. Killian, *Eur. Biophys. J.* **2016**, *45*, 3–21.
[8] J. Radoicic, S. H. Park, S. J. Opella, *Biophys. J.* **2018**, *115*, 22–25.

[9] A. F. Craig, E. E. Clark, I. D. Sahu, R. Zhang, N. D. Frantz, M. S. Al-Abdul-Wahid, C. Dabney-Smith, D. Konkolewicz, G. A. Lorigan, *Biochim. Biophys. Acta.* **2016**, *1858*, 2931 – 2939.
[10] F. Hagn, M. L. Nasr, G. Wagner, *Nat. Protoc.* **2018**, *13*, 79.
[11] M. C. Fiori, Y. Jiang, G. A. Altenberg, H. Liang, *Sci. Rep.* **2017**, *7*, 7432.
[12] S. C. L. Hall, C. Tognoloni, J. Charlton, E. C. Bragginton, A. J. Rothnie, P. Sridhar, M. Wheatley, T. J. Knowles, T. Arnold, K. J. Edler, T. R. Dafforn, *Nanoscale* **2018**, *10*, 10609 – 10619.
[13] Z. Stroud, S. C. L. Hall, T. R. Dafforn, *Methods* **2018**, *147*, 106 – 117.
[14] T. J. Knowles, R. Finka, C. Smith, Y. P. Lin, T. Dafforn, M. Overduin, *J. Am. Chem. Soc.* **2009**, *131*, 7484 – 7485.
[15] T. Ravula, N. Z. Hardin, J. Bai, S. C. Im, L. Waskell, A. Ramamoorthy, *Chem. Commun.* **2018**, *54*, 9615 – 9618.
[16] S. Lindhoud, V. Carvalho, J. W. Pronk, M. E. Aubin-Tam, *Biomacromolecules* **2016**, *17*, 1516 – 1522.
[17] D. J. K. Swainsbury, S. Scheidelaar, N. Foster, R. van Grondelle, J. A. Killian, M. R. Jones, *Biochim. Biophys. Acta.* **2017**, *1859*, 2133 – 2143.
[18] A. Oluwole, B. Danielczak, A. Meister, J. Babalola, C. Vargas, S. Keller, *Angew. Chem. Int. Ed.* **2017**, *56*, 1919 – 1924; *Angew. Chem.* **2017**, *129*, 1946 – 1951.
[19] T. Ravula, S. K. Ramadugu, G. Di Mauro, A. Ramamoorthy, *Angew. Chem. Int. Ed.* **2017**, *56*, 11466 – 11470; *Angew. Chem.* **2017**, *129*, 11624 – 11628; Corrigendum: T. Ravula, S. K. Ramadugu, G. Di Mauro, A. Ramamoorthy, *Angew. Chem. Int. Ed.* **2019**, *58*, 13184 – 13184; *Angew. Chem.* **2019**, *131*, 13318 – 13318.
[20] J. M. Dörr, M. C. Koorengevel, M. Schäfer, A. V. Prokofyev, S. Scheidelaar, E. A. W. van der Cruijsen, T. R. Dafforn, M. Baldus, J. A. Killian, *Proc. Natl. Acad. Sci. USA* **2014**, *111*, 18607 – 18612.
[21] M. Overduin, M. Esmaili, *Appl. Sci.* **2019**, *9*, 1230.
[22] J. F. Bada Juarez, D. O'Rourke, P. J. Judge, L. C. Liu, J. Hodgkin, A. Watts, *Chem. Phys. Lipids* **2019**, *222*, 51 – 58.
[23] T. Ravula, A. Ramamoorthy, *Angew. Chem. Int. Ed.* **2019**, *58*, 14925 – 14928; *Angew. Chem.* **2019**, *131*, 15067 – 15070.
[24] R. Puthenveetil, K. Nguyen, O. Vinogradova, *Nanotechnol. Rev.* **2017**, *6*, 111 – 126.
[25] S. Cai, C. Seu, Z. Kovacs, A. D. Sherry, Y. Chen, *J. Am. Chem. Soc.* **2006**, *128*, 13474 – 13478.
[26] K. Yamamoto, J. Xu, K. E. Kawulka, J. C. Vederas, A. Ramamoorthy, *J. Am. Chem. Soc.* **2010**, *132*, 6929 – 6931.
[27] K. Yamamoto, S. Vivekanandan, A. Ramamoorthy, *J. Phys. Chem. B* **2011**, *115*, 12448 – 12455.
[28] V. Kocman, G. M. Di Mauro, G. Veglia, A. Ramamoorthy, *Solid State Nucl. Magn. Reson.* **2019**, *102*, 36 – 46.
[29] I. Sengupta, M. Gao, R. J. Arachchige, P. S. Nadaud, T. F. Cunningham, S. Saxena, C. D. Schwieters, C. P. Jaroniec, *J. Biomol. NMR* **2015**, *61*, 1 – 6.
[30] G. M. Clore, *Methods Enzymol.* **2015**, *564*, 485 – 497.
[31] E. S. Salnikov, F. Aussenac, S. Abel, A. Purea, P. Tordo, O. Ouari, B. Bechinger, *Solid State Nucl. Magn. Reson.* **2019**, *100*, 70 – 76.
[32] Q. Z. Ni, E. Daviso, T. V. Can, E. Markhasin, S. K. Jawla, T. M. Swager, R. J. Temkin, J. Herzfeld, R. G. Griffin, *Acc. Chem. Res.* **2013**, *46*, 1933 – 1941.
[33] S. V. Dvinskikh, V. Castro, D. Sandström, *Phys. Chem. Chem. Phys.* **2005**, *7*, 607 – 613.
[34] M. M. Hoffmann, H. S. Sobstyl, S. J. Seedhouse, *Magn. Reson. Chem.* **2008**, *46*, 660 – 666.
[35] C. Lin, D. Yang, *Methods Mol. Biol.* **2017**, *1587*, 171 – 196.
[36] N. Niccolai, E. Morandi, S. Gardini, V. Costabile, R. Spadaccini, O. Crescenzi, D. Picone, O. Spiga, A. Bernini, *Biochim. Biophys. Acta Proteins Proteom.* **2017**, *1865*, 201 – 207.
[37] H. G. Hocking, K. Zangger, T. Madl, *ChemPhysChem* **2013**, *14*, 3082 – 3094.
[38] C. Hartlmüller, J. C. Günther, A. C. Wolter, J. Wöhnert, M. Sattler, T. Madl, *Sci. Rep.* **2017**, *7*, 5393.
[39] C. Hartlmüller, E. Spreitzer, C. Göbl, F. Falsone, T. Madl, *J. Biomol. NMR* **2019**, *73*, 305 – 317.
[40] G. Esposito, A. M. Lesk, H. Molinari, A. Motta, N. Niccolai, A. Pastore, *J. Mol. Biol.* **1992**, *224*, 659 – 670.
[41] S. C. Keane, X. Heng, K. Lu, S. Kharytonchyk, V. Ramakrishnan, G. Carter, S. Barton, A. Hosic, A. Florwick, J. Santos, N. C. Bolden, S. McCowin, D. A. Case, B. A. Johnson, M. Salemi, A. Telesnitsky, M. F. Summers, *Science* **2015**, *348*, 917 – 921.
[42] P. Niedbalski, C. Parish, Q. Wang, Z. Hayati, L. Song, A. F. Martins, A. D. Sherry, L. Lumata, *J. Phys. Chem. A* **2017**, *121*, 9221 – 9228.
[43] E. Ravera, D. Shimon, A. Feintuch, D. Goldfarb, S. Vega, A. Flori, C. Luchinat, L. Menichetti, G. Parigi, *Phys. Chem. Chem. Phys.* **2015**, *17*, 26969 – 26978.
[44] J. R. Yarava, S. R. Chaudhari, A. J. Rossini, A. Lesage, L. Emsley, *J. Magn. Reson.* **2017**, *277*, 149 – 153.
[45] R. Rogawski, A. E. McDermott, *Arch. Biochem. Biophys.* **2017**, *628*, 102 – 113.

Manuscript received: August 8, 2019
Revised manuscript received: September 11, 2019
Accepted manuscript online: September 17, 2019
Version of record online: October 17, 2019

